LUND UNIVERSITY

Role of quasiparticle structure in α decay of superheavy nuclei

Clark, R. M.; Rudolph, D.

Role of quasiparticle structure in α decay of superheavy nuclei

R. M. Clark[1] and D. Rudolph [2]

[1]*Nuclear Science Division, Lawrence Berkeley National Laboratory, Berkeley, California 94720, USA*
[2]*Department of Physics, Lund University, 22100 Lund, Sweden*

We use the superfluid tunneling model (STM) to calculate the half-lives of α decays of odd-A and odd-odd superheavy nuclei (SHN) with $Z \geqslant 100$ and $A \geqslant 250$. The experimental data are reproduced to accuracies comparable to other contemporary models of the α decay of the SHN. We then apply the STM to examine the influence of the quasiparticle structure on the properties of the chains of α decays arising from odd-A SHN. Using representative calculations of the one-quasi-particle structure of odd-Z and odd-N SHN, we illustrate the important role played by high-Ω orbitals in defining the observed characteristics of the α-decay chains. We point out sources of possible ambiguity that may arise due to the quasiparticle structure when assigning α-decay chains to specific SHN.

I. INTRODUCTION

New experiments are addressing the fundamental issue of the maximum limit of nuclear mass and charge. Observation of elements with atomic numbers $112 < Z \leqslant 118$, [1–8], has resulted in the completion of the seventh period of the Periodic Table. A common decay mode of the nuclei of these superheavy elements is α decay, which can dominate over other possible decay modes, such as electron capture or fission.

Fine structure observed in the α decay is indicative of population and decay between the ground states and excited states in the parent and daughter isotopes, and often gives the first structural information on the excitations of these nuclei. Notable examples of α-decay fine structure include the case of the even-even (e-e) nucleus ^{270}Ds (darmstadtium, $Z = 110$), which arises from high-K isomers present in nuclei of the α-decay chains [9–11]. Other cases of α-decay fine structure are known in odd-A and odd-odd (o-o) nuclei, where multiple α-decay pathways can lead to different excited states. A prominent example is ^{288}Mc (moscovium, $Z = 115$) [12]. After the initial observation of α-decay fine structure, which indicated population of multiple excited states in nuclei along the decay chains, follow-up studies led to the identification of discrete γ-ray transitions in the decay schemes of ^{276}Mt (meitnerium, $Z = 109$) and ^{272}Bh (bohrium, $Z = 107$) [13,14], placing constraints on the models of quasiparticle structure for these nuclei [15]. Most recently, α-decay fine structure and electromagnetic decays have been observed along the decay chains of odd-A ^{289}Fl (flerovium, $Z = 114$) giving the first information on the excited levels and the one quasineutron structure of these nuclei [16,17].

Theoretically, α decay is usually interpreted as a tunneling process of an α particle, which has preformed near the nuclear surface. There are many phenomenological models [18–31] (and references therein), which treat the decay as though it involves the binary system of the daughter nucleus and the α particle. The subsequent decay process is described in terms

of standard Gamow theory of tunneling through a barrier. Different aspects of the process can be investigated with such models. For instance, the influence of surface diffuseness anisotropies on the decay were investigated recently [32] using an improved cluster model. The STM allows us to examine the role of pairing in the decay process, which is important if one is to understand the role of quasiparticle structure on the α decay of SHN. Specifically, the occurrence and interpretation of α-decay fine structure in the α-decay chains of odd-A and odd-odd SHN requires one to consider three major factors: (i) the energies of the states involved—the larger the Q value of the α decay Q_{α}, the shorter the lifetime; (ii) the angular momentum of the states involved in the decay—a large difference in angular momentum will give rise to a larger centrifugal barrier resulting in a longer lifetime; (iii) the role of the odd particle(s) on the pairing correlations. The superfluid tunneling model (STM) [33–35] enables us to examine the influence of each of these factors on the α decay of odd-A and odd-odd SHN.

Previously [36], it was shown that the STM could be applied to the description of α decay of the ground state and multiquasiparticle states across different regions of the nuclear chart from the neutron-deficient $A \sim 150$ region up through the heavy actinide region. In another study [37], we applied the STM to compare against the experimental data on all known even-even SHN with $100 \leqslant Z \leqslant 118$, isotopes of fermium ($Z = 100$) to oganesson ($Z = 118$). Remarkable quantitative agreement, comparable to the fits of recent empirical parametrizations, was found. Notably, we were also able to reproduce the features of the observed fine structure in the α decay from the high-K isomer in ^{270}Ds [9–11,37].

In this article, we apply the STM to a systematic investigation of the α decay of odd-A and odd-odd SHN with $Z \geqslant 100$ and $A \geqslant 250$. Once again, we find that the experimental data are reproduced to accuracies comparable to, or better than, other contemporary models of α decay of the SHN. We apply the STM to examine the influence of the quasiparticle

TABLE I. Comparison between the decimal logarithms of the experimental and calculated α-decay half-lives (in seconds) for the known odd-A and odd-odd SHN with $Z \geqslant 100$ and $A \geqslant 250$. The first column gives the nucleus of interest. The superscripts [a,b] indicate if a second α-decaying state in the parent nucleus has been included in the analysis. The second column gives the Q value for the α decay, Q_α (in MeV with uncertainties typically less than 0.5% of the absolute value) corresponding to the strongest α-decay branch, taken from the evaluated nuclear data files [43] or from Refs. [7,8,16,17,44–47]. The experimental α-decay branching ratio is taken into account. The third column has the decimal logarithm of the experimental half-life again from Refs. [7,8,16,17,43–47]. Generally, the experimental uncertainties in the half-lives are small enough to be ignored but are included as error bars in Figs. 1–3 for completeness. The fourth–sixth columns are the decimal logarithms of the α-decay half-lives calculated using the superfluid tunneling model ($T_{1/2,\,\mathrm{STM}}$), the Viola-Seaborg formula [39,40] ($T_{1/2,\,\mathrm{VS}}$), and the Royer formula [41] ($T_{1/2,\,\mathrm{Royer}}$), respectively.

Nucleus	Q_α (MeV)	$\log_{10}(T_{1/2,\mathrm{expt}})$ (s)	$\log_{10}(T_{1/2,\mathrm{STM}})$ (s)	$\log_{10}(T_{1/2,\mathrm{VS}})$ (s)	$\log_{10}(T_{1/2,\mathrm{Royer}})$ (s)
		Odd-A (even-Z, odd-N)			
^{251}Fm	6.945	6.09	6.39	6.30	6.42
^{253}Fm	7.055	6.71	6.05	5.85	5.89
^{255}Fm	7.134	4.89	5.48	5.52	5.51
^{257}Fm	6.623	6.97	7.73	7.69	7.79
^{251}No[a]	8.750	0.02	0.50	0.69	0.48
^{251}No[b]	8.808	0.02	0.32	0.52	0.29
^{253}No	8.132	2.23	2.53	2.66	2.54
^{255}No	8.224	2.72	2.35	2.35	2.18
^{257}No	8.352	1.54	1.68	1.93	1.69
^{259}No	7.623	3.67	4.29	4.45	4.35
^{255}Rf	8.855	0.58	0.88	1.10	0.89
^{257}Rf[a]	8.908	0.84	0.85	0.94	0.68
^{257}Rf[b]	9.083	0.75	0.12	0.43	0.13
^{259}Rf	9.01	0.50	0.23	0.64	0.32
^{261}Rf[a]	8.41	1.88	2.22	2.49	2.27
^{261}Rf[b]	8.65	0.85	1.40	1.72	1.44
^{259}Sg	9.76	−0.49	−1.08	−0.76	−1.13
^{261}Sg	9.56	−0.74	−0.59	−0.21	−0.58
^{263}Sg	9.23	0.03	0.33	0.70	0.36
^{265}Sg[a]	8.98	0.97	1.07	1.45	1.13
^{265}Sg[b]	8.82	1.26	1.56	1.91	1.62
^{269}Sg	8.70	2.08	1.88	2.30	1.96
^{271}Sg	8.67	2.28	1.94	2.40	2.03
^{263}Hs	10.71	−2.92	−2.96	−2.47	−3.00
^{265}Hs[a]	10.46	−2.72	−2.39	−1.86	−2.39
^{265}Hs[b]	10.70	−3.52	−3.00	−2.45	−3.01
^{267}Hs	10.00	−1.28	−1.22	−0.72	−1.19
^{269}Hs	9.27	0.99	0.85	1.29	0.93
^{273}Hs	9.73	−0.70	−0.60	−0.01	−0.54
^{275}Hs	9.45	−0.66	0.18	0.78	0.27
^{269}Ds	11.30	−3.57	−3.82	−3.18	−3.83
^{271}Ds	10.89	−2.79	−2.90	−2.26	−2.88
^{273}Ds	11.29	−3.72	−3.87	−3.15	−3.87
^{277}Ds	10.72	−2.22	−2.60	−1.87	−2.57
^{279}Ds	9.87	0.29	−0.32	0.34	−0.22
^{281}Ds	8.75	2.28	2.73	3.24	2.87
^{277}Cn	11.38	−3.21	−3.51	−2.76	−3.49
^{281}Cn	10.45	−0.89	−1.28	−0.56	−1.18
^{283}Cn	9.67	0.73	0.87	1.52	1.02
^{285}Cn	9.20	1.62	1.90	2.52	2.07
^{285}Fl	10.56	−0.82	−0.95	−0.19	−0.82
^{287}Fl	10.16	−0.32	0.06	0.80	0.23
^{289}Fl	9.94	0.40	0.79	1.33	0.75
^{291}Lv	10.90	−1.72	−1.24	−0.38	−1.08
^{293}Lv	10.69	−1.02	−0.94	0.07	−0.63

TABLE I. (*Continued.*)

Nucleus	Q_α (MeV)	$\log_{10}(T_{1/2,\text{expt}})$ (s)	$\log_{10}(T_{1/2,\text{STM}})$ (s)	$\log_{10}(T_{1/2,\text{VS}})$ (s)	$\log_{10}(T_{1/2,\text{Royer}})$ (s)
		Odd-*A* (odd-*Z*, even-*N*)			
[251]Md	7.672	3.41	3.83	3.67	3.79
[253]Md	7.217	4.71	5.63	5.40	5.58
[255]Md	7.430	4.31	4.71	4.57	4.68
[257]Md	7.186	5.12	5.67	5.52	5.65
[253]Lr[a]	8.859	0.12	0.51	0.52	0.54
[253]Lr[b]	8.927	−0.17	0.30	0.32	0.32
[255]Lr[a]	8.498	1.59	1.64	1.63	1.67
[255]Lr[b]	8.592	0.83	1.33	1.34	1.36
[257]Lr	8.950	−0.69	0.14	0.25	0.19
[259]Lr	8.484	0.90	1.59	1.67	1.65
[255]Db	8.859	0.30	1.26	1.24	1.35
[257]Db[a]	9.313	−0.44	-0.18	−0.08	−0.08
[257]Db[b]	9.206	0.40	0.14	0.22	0.24
[259]Db	9.62	−0.29	−1.10	−0.92	−1.00
[261]Db	9.07	0.23	0.47	0.62	0.60
[263]Db	8.49	1.82	2.31	2.40	2.45
[261]Bh	10.16	−1.93	−1.88	−1.65	−1.71
[265]Bh	9.38	−0.03	0.21	0.41	0.41
[267]Bh	8.96	1.23	1.46	1.64	1.67
[271]Bh	9.45	0.26	−0.03	0.31	0.20
[275]Mt	10.49	−1.68	−2.30	−1.81	−2.02
[279]Rg	10.53	−1.03	−1.81	−1.29	−1.44
[281]Rg	9.41	2.15	1.32	1.70	1.70
[283]Nh	10.32	−1.09	−0.79	−0.26	−0.33
[285]Nh	10.01	0.62	0.20	0.70	0.67
[287]Mc	10.78	−1.38	−1.17	−0.58	−0.65
[289]Mc	10.49	−0.48	−0.49	0.11	0.06
[293]Ts	11.32	−1.66	−2.02	−1.31	−1.43
		Odd-*Z*, odd-*N*			
[250]Md	7.97	2.85	3.26	3.22	3.31
[256]Md	7.320	4.90	5.64	5.58	5.81
[258]Md	6.824	6.83	7.77	7.62	8.01
[252]Lr	9.150	−0.57	0.13	0.27	0.11
[254]Lr	8.595	1.43	1.84	1.92	1.89
[256]Lr	8.564	1.92	1.89	2.01	1.96
[258]Lr	8.756	0.94	1.22	1.42	1.28
[260]Lr	8.161	2.35	3.20	3.32	3.34
[256]Db	9.157	0.57	0.81	0.95	0.87
[258]Db	9.341	0.45	0.21	0.42	0.26
[260]Db	9.183	0.48	0.64	0.87	0.72
[262]Db	8.591	2.00	2.49	2.66	2.65
[270]Db	8.02	3.68	4.35	4.56	4.62
[260]Bh	10.32	−1.46	−1.80	−1.47	−1.79
[264]Bh	9.69	−0.36	−0.14	0.14	−0.08
[266]Bh	9.56	0.32	0.15	0.50	0.29
[270]Bh	9.06	1.79	1.59	1.93	1.80
[272]Bh	9.21	1.02	1.07	1.49	1.28
[274]Bh	8.94	1.64	1.88	2.30	2.13
[266]Mt	11.00	−2.77	−2.92	−2.44	−2.89
[268]Mt	10.322	−1.15	−1.26	−0.83	−1.14
[270]Mt	10.18	−0.32	−0.92	−0.47	−0.78
[274]Mt	9.91	−0.36	−0.26	0.25	−0.06
[276]Mt	10.10	−0.17	−0.84	−0.26	−0.66
[278]Mt	9.58	0.65	0.60	1.13	0.85
[272]Rg	11.15	−2.42	−2.72	−2.16	−2.61

TABLE I. (*Continued.*)

Nucleus	Q_α (MeV)	$\log_{10}(T_{1/2,\text{expt}})$ (s)	$\log_{10}(T_{1/2,\text{STM}})$ (s)	$\log_{10}(T_{1/2,\text{VS}})$ (s)	$\log_{10}(T_{1/2,\text{Royer}})$ (s)
^{274}Rg	11.20	−1.92	−2.89	−2.27	−2.77
^{278}Rg	10.85	−2.38	−2.12	−1.47	−1.95
^{280}Rg	10.16	0.64	−0.36	0.24	−0.09
^{282}Rg	9.16	2.00	2.64	3.04	2.98
^{278}Nh	11.84	−2.85	−3.77	−3.06	−3.64
^{282}Nh	10.78	−1.14	−1.33	−0.67	−1.06
^{284}Nh	10.20	−0.01	0.18	0.79	0.52
^{286}Nh	9.79	0.98	1.32	1.90	1.72
^{288}Mc	10.70	−0.77	−0.54	0.15	−0.17
^{290}Mc	10.41	−0.19	0.20	0.89	0.61
^{294}Ts	11.18	−1.29	−1.20	−0.38	−0.79

structure on the properties of the chains of α decays arising from odd-*A* SHN. Using representative calculations, of the one-quasi-particle structure of nuclei in the decay chains originating from ^{289}Mc, and ^{293}Lv (livermorium, $Z = 116$), we illustrate the important role played by opposite-parity high-Ω orbitals in defining the observed characteristics. We point out sources of possible ambiguity that may arise due to the quasi-particle structure when assigning α-decay chains to specific SHN.

The STM and its application have been discussed in detail elsewhere [33–38]. For completeness, we describe the main features of the model in the Appendix. In Sec. II, we compare the results of the model with the known experimental data on odd-*A* and odd-odd SHN and with the results of other models for the α decay of the SHN. In Sec. III, we present the results on the α-decay chains of ^{289}Mc and ^{293}Lv, using available structure calculations in order to qualitatively illustrate the influence of the quasiparticle structure on α decay and the possibility of ambiguities of assigning observed α-decay chains to specific isotopes. Conclusions are presented in Sec. IV, which is followed by a short summary.

II. α DECAYS OF ODD-*A* AND ODD-ODD SHN

Previously [37], we used the STM to calculate the ground-state-to-ground-state decays for known α-decaying even-even SHN. By focusing on the even-even systems, we eliminated ambiguities in Q_α and L, which might arise due to possible excitations of either the parent or the daughter nucleus. The data were reproduced to within about a factor of 3, which is an accuracy comparable to that from empirical-fitting approaches including the Viola-Seaborg (VS) formula [39] (fitted as described in Ref. [40]) and the Royer formula (as described in Ref. [41]). This was taken to indicate that the STM contains all the physical ingredients necessary for a quantitative description of the α decay of even-even SHN [37].

To perform a systematic study, using the STM of the odd-*A* and odd-odd SHN with $Z \geqslant 100$ and $A \geqslant 250$, we have taken the measured α-particle energy E_α of the strongest branch observed (in many cases, only one branch has been seen or assigned) and converted it to an associated Q_α value to be used in the calculation. In most cases, except where explicitly stated in the literature to be otherwise, the initial and final

states are assumed to have the same spin and parity, implying that $L = 0$. In regions of deformation, it is known that such decays are "favored" to occur between states in odd-*A* nuclei with the same Nilsson quantum numbers [42]. The situation may be more complicated for cases of odd-odd nuclei. As noted in Ref. [36], reduction of pairing from blocking by the odd particle(s) must be taken into account. It was found that by reducing the pairing gap parameter to 90% of its standard value such that $\Delta_o = 0.9 \times \Delta$, where $\Delta = 12 A^{-1/2}$ MeV, one is able to reproduce the data on known α decays of the odd-*A* SHN. Reducing the pairing gap parameter to 80% of the value of $\Delta_{o-o} = 0.8 \times \Delta$, enables one to reproduce the α decays of the odd-odd SHN.

In Table I, we present the results of our calculations in comparison to experimental data. Figure 1 shows that ex-

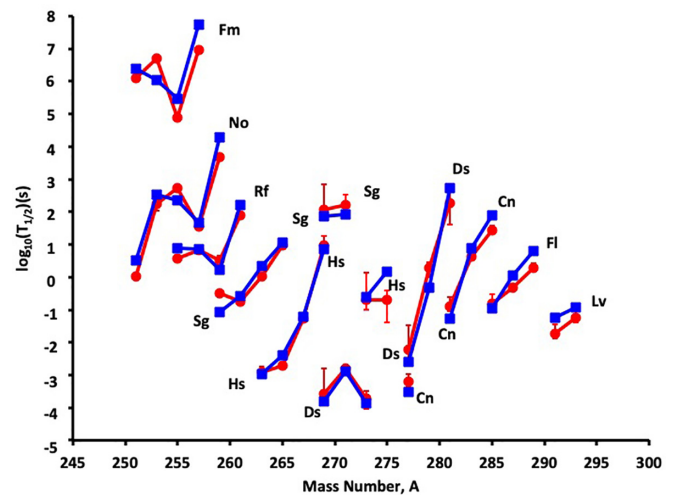FIG. 1. Decimal logarithm of α-decay half-lives (in seconds) of odd-*A* (even-*Z*, odd-*N*) isotopes with $Z \geqslant 100$ as a function of nuclear mass number A. The experimental data are marked with (red) circles (except where seen, errors are typically less than the size of the symbol—see comment in the caption of Table I). The results of the calculations from the STM are shown as filled (blue) squares. The data points for neighbors in isotope chains indicated with the corresponding element symbol are joined by solid lines to guide the eye.
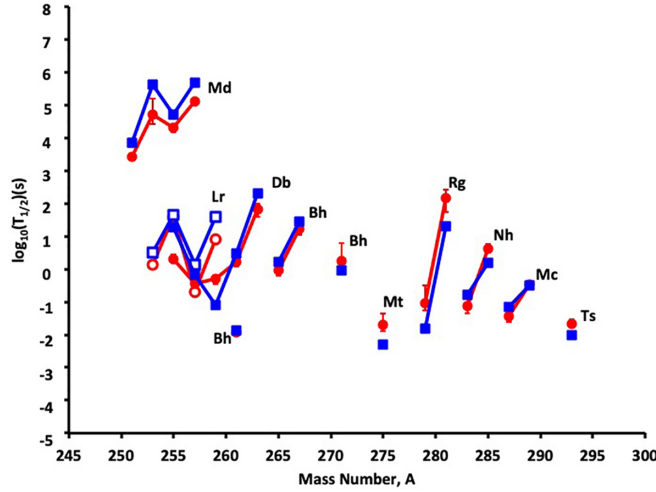
FIG. 2. The same as Fig. 1 but for odd-*A* (odd-*Z*, even-*N*) isotopes with $Z > 100$. For clarity, open symbols are used for the Lr isotopes, whereas closed symbols are used for the Db isotopes.

FIG. 4. Decimal logarithms of the ratios between the experimental and the theoretical half-lives for the odd-*Z* odd-*N* SHN with $Z > 100$. The open circles are the values when the pairing gap parameter is taken as $\Delta_{o-o} = \Delta_{e-e} = \Delta = 12\,A^{-1/2}$ MeV. The solid circles are the results when the pairing gap parameter is reduced such that $\Delta_{o-o} = 0.8 \times \Delta_{e-e}$. The dashed lines are simply to guide the eye and show order-of-magnitude differences in the calculated half-lives.

perimental α-decay half-lives compared to the results of our calculations for odd-*A* SHN with odd-*N*, whereas Fig. 2 is for the odd-*A* SHN with odd-*Z*. Figure 3 is the comparison for the odd-odd SHN. One can see that the experimental α-decay half-lives, which extend across roughly 12 orders of magnitude, are well reproduced by the STM. In Fig. 4 we have plotted the decimal logarithms of the ratios between the experimental and the theoretical half-lives for all the odd-odd SHN with and without reducing Δ. One can immediately see the importance of taking into account the reduced Δ in order to reproduce the α-decay half-lives of the odd-odd SHN.

In Table I, we also include the predictions of the two different empirical-fitting approaches for comparison, namely, the Viola-Seaborg formula [39,40] and the Royer formula [41]. For a quantitative comparison between the models, a common approach is to calculate the average of the absolute values of
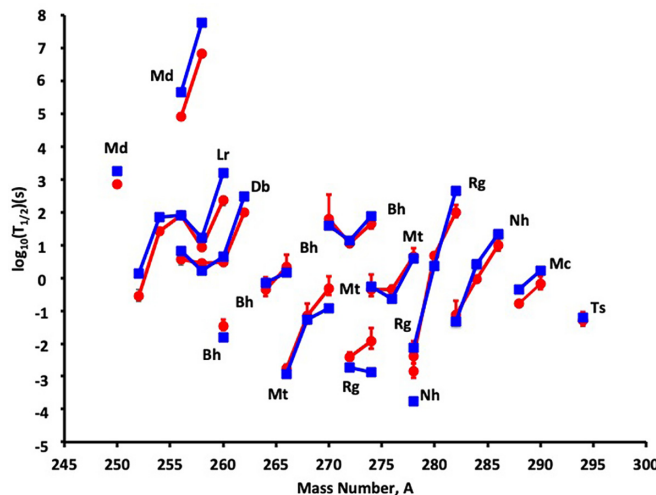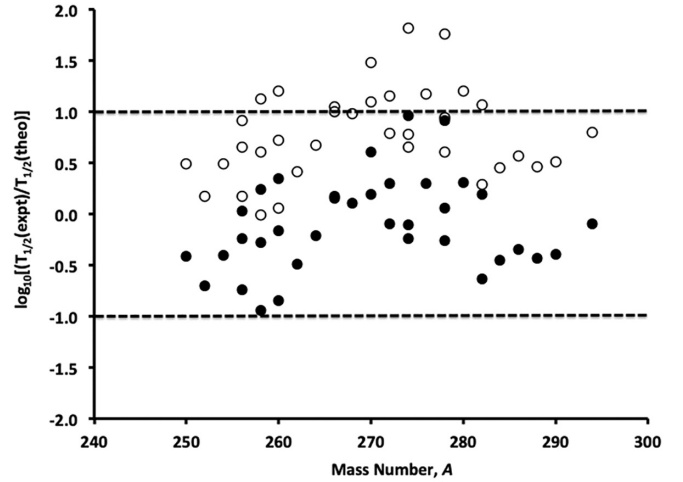
the differences in the decimal logarithms given as

$$\delta = \frac{1}{N} \sum_{k=1}^{N} \left| \log_{10}\left(\frac{T_{1/2,\text{expt},k}}{T_{1/2,\text{theo},k}} \right) \right|. \qquad (1)$$

For the different approaches used in this paper, we find the values of δ as presented in Table II for the subsets of the SHN with even-*Z*-odd-*N* (e-o), odd-*Z*-even-*N* (o-e), and odd-*Z*-odd-*N* (o-o), calculated using the superfluid tunneling model, the Viola-Seaborg formula, and the Royer formula, respectively. For completeness, we also give the values of δ as previously determined [37] for the subset of SHN with even-*Z*-even-*N* (e-e). We conclude that the superfluid tunneling model is able to reproduce the experimental data on the α decay of SHN to about the same level of accuracy as contemporary empirical formulas.

FIG. 3. The same as Fig. 1 but for odd-*Z*, odd-*N* isotopes with $Z > 100$.

TABLE II. Comparison between the averages of the absolute values of the differences in the decimal logarithms δ as defined by Eq. (1) and calculated for the subsets of the SHN with even-*Z*-even-*N* (e-e), even-*Z*-odd-*N* (e-o), odd-*Z*-even-*N* (o-e), and odd-*Z*-odd-*N* (o-o) for the STM, the Viola-Seaborg formula (VS), and the Royer formula as described in the text.

$Z-N$	STM	VS	Royer
e-e	0.22	0.26	0.19
e-o	0.35	0.62	0.38
o-e	0.45	0.45	0.47
o-o	0.38	0.54	0.46

TABLE III. The predicted excitation energies of one-quasi-proton states in ^{289}Mc, ^{285}Nh, and ^{281}Rg from calculations using a self-consistent SEDF approach with the UNEDF1 parametrization [15] from a Nilsson-model approach [15,45,48], and from a Woods-Saxon model [49]. The levels are labeled with asymptotic Nilsson quantum numbers.

Nucleus	SEDF-UNEDF1		Nilsson		Woods-Saxon	
	Orbital	Energy (MeV)	Orbital	Energy (MeV)	Orbital	Energy (MeV)
^{289}Mc	$[503]7/2^-$	0.00	$[521]1/2^-$	0.00	$[541]1/2^-$	0.00
	$[512]3/2^-$	0.02	$[512]3/2^-$	0.15	$[512]3/2^-$	0.06
	$[510]1/2^-$	0.09	$[510]1/2^-$	0.38	$[606]13/2^+$	0.16
	$[615]11/2^+$	0.27	$[503]7/2^-$	0.66	$[503]7/2^-$	0.29
	$[550]1/2^-$	0.44	$[606]13/2^+$	0.69	$[510]1/2^-$	0.36
^{285}Nh	$[510]1/2^-$	0.00	$[606]13/2^+$	0.00	$[512]3/2^-$	0.00
	$[512]3/2^-$	0.04	$[503]7/2^-$	0.05	$[510]1/2^-$	0.15
	$[615]11/2^+$	0.09	$[615]11/2^+$	0.23	$[503]7/2^-$	0.15
	$[505]9/2^-$	0.29	$[512]3/2^-$	0.35	$[550]1/2^-$	0.15
	$[550]1/2^-$	0.41	$[624]9/2^+$	0.41	$[615]11/2^+$	0.45
^{281}Rg	$[615]11/2^+$	0.00	$[606]13/2^+$	0.00	$[615]11/2^+$	0.00
	$[512]3/2^-$	0.02	$[503]7/2^-$	0.01	$[521]1/2^-$	0.08
	$[505]9/2^-$	0.09	$[615]11/2^+$	0.16	$[505]9/2^-$	0.16
	$[510]1/2^-$	0.22	$[512]3/2^-$	0.38	$[512]3/2^-$	0.20
	$[521]1/2^-$	0.60	$[521]1/2^-$	0.39	$[503]7/2^-$	0.39

III. ROLE OF QUASIPARTICLE STRUCTURE IN α DECAY CHAINS

Having shown that the STM seems to contain all the necessary physical ingredients to reproduce the major features of the α decay of the SHN, we now apply the model to the case of the α-decay chains of odd-A SHN. We will look at representative cases for odd-Z and odd-N systems.

For an odd-Z case, we examine differences in properties of the α-decay chains arising from the predictions of the one-quasi-proton structure for the decay chains of ^{289}Mc ($Z = 115$, $N = 174$) as calculated using three different models. The first is a locally optimized self-consistent Skyrme energy density functional (SEDF) with the UNEDF1 parametrization as described in Ref. [15]. The second uses a microscopic-macroscopic Nilsson-model approach described in Refs. [15,45,48]. The third set of calculations uses a Woods-Saxon potential [49].

For the odd-N case, we examine the decay chains of ^{293}Lv ($Z = 116$, $N = 177$) as calculated by Ćwiok *et al.* [50]. The calculations use the Hartree-Fock-Bogoliubov (HFB) method with the SLy4 Skyrme effective interaction. The HFB + SLy4 prescription is widely used for calculations of properties of the SHN [51,52], and the calculations in Ref. [50] provide extensive information on the lowest one-quasi-neutron excitation in the relevant nuclei.

For the decay chains of ^{289}Mc, the predicted excitation energies of low-lying one-quasi-proton states in ^{289}Mc, ^{285}Nh, and ^{281}Rg from calculations using the SEDF-UNEDF1, the Nilsson model, and the Woods-Saxon model are reproduced in Table III. We use the asymptotic Nilsson quantum numbers as a labeling notation. One sees that there are often several negative-parity states arising from the $\mathcal{N} = 5$ major shell lying at relatively low energy. One can also see that another feature of the models is that it often occurs that, at least, one high-Ω

positive-parity state from the $\mathcal{N} = 6$ major shell can lie at relatively low excitation energy. Such a state is likely to be isomeric [45]. Since all these states will be populated in the initial compound nucleus reaction forming ^{289}Mc, we might reasonably expect α decays from, at least, one of the low-lying negative-parity orbitals and from the high-Ω positive-parity state.

In order to study the influence of the one-quasi-proton structure on the resulting α-decay fine structure, we use the STM to calculate the strongest branches from the ground state and possible excited isomeric states for each nucleus in the decay chain. We use the prescription discussed above with the pairing parameter taken with the reduced value of $\Delta_o = 0.9 \times \Delta$, and accounting for the angular momentum L of the transition by assuming that it takes the lowest value given by the selection rules $|I_i - I_f| \leqslant L \leqslant I_i + I_f$ and $\pi_i = (-1)^L \pi_f$, where $I_i(I_f)$ and $\pi_i(\pi_f)$ correspond to the angular momentum and parity of the initial (final) state involved in the decay, respectively. If multiple states are populated, we assume a fast electromagnetic decay to a lower-lying state if an $E1$, $M1$, or $E2$ transition is allowed. Note, it is known that low-lying rotational band members built on Nilsson states are populated in α decay [53–56], but we are not taking this additional complication explicitly into account. The energies of the α decays use the Q_α values in Table I, assumed to correspond to the ground-state-to-ground-state transition and account for the excitation energy of the one-quasi-proton states in both parent and daughter. The results of the calculations are presented in Table IV.

One sees several interesting features. The decay step from ^{289}Mc $\rightarrow$ ^{285}Nh has several competing α transitions from both the ground and the excited isomeric state as predicted by SEDF-UNEDF1 calculation. However, differences in Q_α values and angular momenta L for these transitions are such that the partial decay constants, and, therefore, the predicted

TABLE IV. Predictions for the dominant transitions (defined as the $>10\%$ branch from a given state) in the α-decay chains of ^{289}Mc $\rightarrow$ ^{285}Nh $\rightarrow$ ^{281}Rg using the SEDF-UNEDF1 (upper part), Nilsson (middle part), or Woods-Saxon (lower part) calculations as discussed in the text. Transitions are labeled using the initial (final) Nilsson orbit in the parent (daughter) nucleus. The fourth column gives the Q value for the α decay, Q_α (in MeV), used in the calculation (estimated from the empirical values in Table I and the excitation energies of states in Table III). The fifth column gives the angular momentum change involved in the transition L. The sixth column gives the resulting partial decay constant for the transition λ (s^{-1}), calculated using the STM.

Parent nucleus	Initial orbital	Final orbital	Q_α (MeV)	L	λ (s^{-1})
		SEDF-UNEDF1			
^{289}Mc	$[503]7/2^-$	$[510]1/2^-$	10.49	4	6.14×10^{-1}
	$[503]7/2^-$	$[512]3/2^-$	10.45	2	1.15×10^{0}
	$[503]7/2^-$	$[615]11/2^+$	10.40	3	5.76×10^{-1}
	$[615]11/2^+$	$[510]1/2^-$	10.76	5	1.74×10^{0}
	$[615]11/2^+$	$[512]3/2^-$	10.72	5	1.36×10^{0}
	$[615]11/2^+$	$[615]11/2^+$	10.67	0	6.53×10^{0}
	$[615]11/2^+$	$[505]9/2^-$	10.47	1	1.68×10^{0}
^{285}Nh	$[510]1/2^-$	$[615]11/2^+$	10.01	5	6.43×10^{-2}
	$[510]1/2^-$	$[512]3/2^-$	9.99	2	2.61×10^{-1}
	$[510]1/2^-$	$[505]9/2^-$	9.92	4	6.67×10^{-2}
	$[510]1/2^-$	$[510]1/2^-$	9.79	0	1.00×10^{-1}
	$[615]11/2^+$	$[615]11/2^+$	10.10	0	7.87×10^{-1}
	$[615]11/2^+$	$[505]9/2^-$	10.01	1	3.84×10^{-1}
		Nilsson			
^{289}Mc	$[521]1/2^-$	$[503]7/2^-$	10.43	4	4.22×10^{-1}
	$[521]1/2^-$	$[512]5/2^-$	10.13	2	1.47×10^{-1}
	$[606]13/2^+$	$[606]13/2^+$	11.03	0	1.29×10^{2}
^{285}Nh	$[503]7/2^-$	$[503]7/2^-$	10.05	0	5.67×10^{-1}
	$[606]13/2^+$	$[606]13/2^+$	10.01	0	4.37×10^{-1}
		Woods-Saxon			
^{289}Mc	$[541]1/2^-$	$[512]3/2^-$	10.49	2	1.48×10^{0}
	$[541]1/2^-$	$[510]1/2^-$	10.34	0	8.41×10^{-1}
	$[541]1/2^-$	$[503]7/2^-$	10.34	4	2.38×10^{-1}
	$[606]13/2^+$	$[512]3/2^-$	10.65	5	8.90×10^{-1}
	$[606]13/2^+$	$[503]7/2^-$	10.50	3	1.08×10^{0}
	$[606]13/2^+$	$[615]11/2^+$	10.20	2	2.33×10^{-1}
^{285}Nh	$[512]3/2^-$	$[521]1/2^-$	9.93	2	1.75×10^{-1}
	$[512]3/2^-$	$[512]3/2^-$	9.81	0	1.15×10^{-1}
	$[615]11/2^+$	$[615]11/2^+$	10.46	0	7.63×10^{0}

half-lives are rather similar. One would, therefore, observe several α-decay lines of different energies, but it would be difficult to distinguish the initial and final states involved. This contrasts with the calculations accounting for the one-quasi-proton structure predicted by the Nilsson model. In that case, the decay step from ^{289}Mc $\rightarrow$ ^{285}Nh has fewer competing α transitions, and the properties are rather different depending on whether the initial state in ^{289}Mc is either the $[521]1/2^-$ ground state or the $[606]13/2^+$ isomer. The $[606]13/2^+$ isomer decays via a single transition with a half-life that will be nearly three orders of magnitude faster than the transitions from the $[521]1/2^-$ ground state and with an energy more than 0.5 MeV higher. A similar effect is seen in the second decay step ^{285}Nh $\rightarrow$ ^{281}Rg predicted by the Woods-Saxon calculations. The isomeric $[615]11/2^+$ state in ^{285}Nh decays via a single transition with an energy 0.5 MeV higher and, at least, an order of magnitude faster than decays from the $[512]3/2^-$ ground state.

The significant differences in properties of the α decay discussed above reflect the differences in the one-quasi-proton structure predicted by the different models. It is our hope that it may eventually be possible to discriminate between the different theoretical frameworks, even with the rather limited experimental information available from α-decay chains of the SHN.

For the odd-N case of ^{293}Lv, the predicted excitation energies of one-quasi-neutron states in ^{293}Lv, ^{289}Fl, ^{285}Cn, ^{281}Ds, and ^{277}Hs from HFB-SLy4 calculations [50] are reproduced in Table V. We find that the low-lying ($\leqslant 1$ MeV) one-quasi-neutron excitations in ^{293}Lv involve several positive-parity orbitals lying close to the Fermi surface, including the $[604]7/2^+$, $[602]5/2^+$, and $[611]1/2^+$ states as the three lowest one-quasi-neutron excitations. Again, one finds that a high-Ω state of opposite (negative) parity, namely, $[707]15/2^-$, also lies below 1 MeV, and it is likely to be isomeric. This one-quasi-neutron structure will influence

TABLE V. The predicted excitation energies of one-quasi-neutron states in ^{293}Lv, ^{289}Fl, ^{285}Cn, ^{281}Ds, and ^{277}Hs from HFB-SLy4 calculations [50] as discussed in the text.

Nucleus	Orbital	Energy (MeV)	Nucleus	Orbital	Energy (MeV)
^{293}Lv	$[604]7/2^+$	0.00	^{281}Ds	$[604]9/2^+$	0.00
	$[602]5/2^+$	0.31		$[606]11/2^+$	0.07
	$[611]1/2^+$	0.52		$[611]1/2^+$	0.12
	$[707]15/2^-$	0.93		$[611]3/2^+$	0.59
^{289}Fl	$[707]15/2^-$	0.00		$[613]5/2^+$	0.65
	$[611]1/2^+$	0.52		$[716]13/2^-$	0.94
	$[604]7/2^+$	0.79	^{277}Hs	$[611]1/2^+$	0.00
	$[602]5/2^+$	1.17		$[604]9/2^+$	0.04
^{285}Cn	$[611]1/2^+$	0.00		$[613]5/2^+$	0.31
	$[611]3/2^+$	0.60		$[716]13/2^-$	0.36
	$[707]15/2^-$	0.62		$[611]3/2^+$	0.38
	$[606]11/2^+$	0.65			
	$[604]9/2^+$	0.72			

the observed α decays, and we again used the STM to calculate the strongest branches from the ground state and possible excited isomeric states for each nucleus in the decay chain using the prescription discussed above. The results of the calculations are presented in Table VI.

In the first step of the decay chain from ^{293}Lv $\rightarrow$ ^{289}Fl, there are two possible α decays to the $[707]15/2^-$ ground state of ^{289}Fl either from the ^{293}Lv $[604]7/2^+$ ground state or from the $[707]15/2^-$ isomeric state (see Table VI). These two possible transitions differ by nearly 1 MeV in energy and involve substantially different changes in angular momentum between initial and final states, resulting in the relative half-lives differing by approximately three orders of magnitude. For the second step in the decay chain from ^{289}Fl $\rightarrow$ ^{285}Cn, there are also two possible transitions. Again, they differ substantially in energy but because of angular momentum hindrance of the higher-energy transition the two lifetimes are rather similar resulting in two competing α-decay branches

from the same parent state. The characteristics of the third and fourth steps in the α-decay chains depend on which state is populated in the second step, but characteristics of these α decays (see Table VI) can be rather different.

IV. CONCLUSIONS

There is a potential for significant ambiguity in assigning α decays to a specific odd-A superheavy isotope. In particular, the presence of isomeric states can result in multiple-α transitions with very different properties being involved in the decay of the same isotope. We have seen this is true for both the odd-Z and odd-N examples discussed above. The interplay between α-decay energies and differences in angular momentum can result in cases where transitions can have different decay energies but similar lifetimes (^{289}Mc as an odd-Z example and ^{289}Fl as an odd-N example—see Tables IV and VI). The reverse situation of very similar energies but

TABLE VI. Predictions for the dominant transitions in the α-decay chains of ^{293}Lv $\rightarrow$ ^{289}Fl $\rightarrow$ ^{285}Cn $\rightarrow$ ^{281}Ds $\rightarrow$ ^{277}Hs using the HFB-SLy4 calculations [50] as discussed in the text. Transitions are labeled using the initial (final) Nilsson orbits in the parent (daughter) nuclei. The fourth column gives the Q value for the α-decay Q_α (in MeV), used in the calculation (estimated from the empirical values in Table I and the excitation energies of states in Table V). The fifth column gives the angular momentum change involved in the transition L. The sixth column gives the resulting partial decay constant for the transition λ (s^{-1}), calculated using the STM.

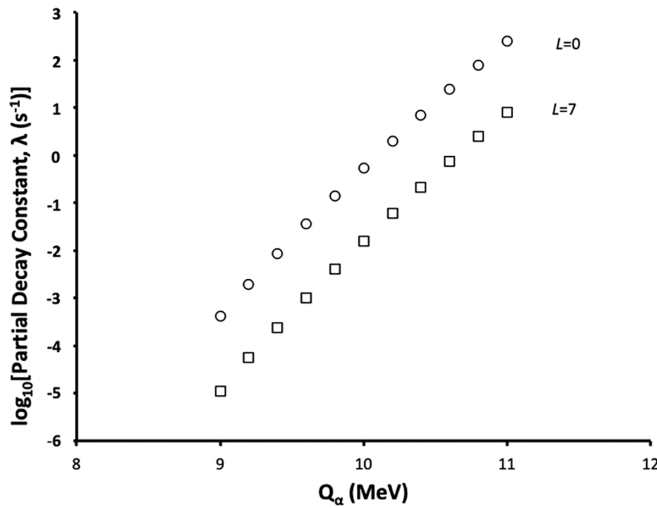|	HFB-SLy4				
Parent nucleus	Initial orbital	Final orbital	Q_α (MeV)	L	λ (s^{-1})
^{293}Lv	$[604]7/2^+$	$[707]15/2^-$	10.69	5	6.16×10^{-1}
	$[707]15/2^-$	$[707]15/2^-$	11.63	0	8.49×10^{2}
^{289}Fl	$[707]15/2^-$	$[611]1/2^+$	9.97	7	5.03×10^{-3}
	$[707]15/2^-$	$[707]15/2^-$	9.34	0	2.06×10^{-3}
^{285}Cn	$[611]1/2^+$	$[604]9/2^+$	9.33	4	2.55×10^{-3}
	$[611]1/2^+$	$[611]1/2^+$	9.21	0	3.90×10^{-3}
	$[707]15/2^-$	$[604]9/2^+$	9.96	3	3.38×10^{-1}
	$[707]15/2^-$	$[606]11/2^+$	9.89	3	2.13×10^{-1}
^{281}Ds	$[604]9/2^+$	$[604]9/2^+$	8.81	0	9.45×10^{-4}
	$[611]1/2^+$	$[611]1/2^+$	8.97	0	3.23×10^{-3}

FIG. 5. Plot of the decimal logarithm of the partial decay constant $\lambda = (\ln 2/T_{1/2})$ in s^{-1} as a function of the Q_α value in MeV, calculated for a nominal α-decay transition from a ^{289}Fl parent nucleus and assuming a difference in angular between the parent and the daughter states of either $L = 0$ (open circles) or $L = 7$ (open squares).

very different lifetimes could also occur. To see these effects more clearly, in Fig. 5, we plot the decimal logarithm of the partial decay constant, λ (s^{-1}), as a function of the Q_α value in MeV, calculated for nominal α-decay transitions from a ^{289}Fl parent nucleus and assuming a difference in angular momentum between the parent and the daughter states of either $L = 0$ or $L = 7$. At a fixed value of Q_α, the difference in angular momentum $\Delta L = 7$ results in the predicted partial decay constant (and, consequently, the extracted lifetime of the transition) differing by over a factor of 30. For a given lifetime, a change in transition energy of about 500 keV will compensate the large difference in angular momentum.

Another ambiguity arises when studying the α decay of the nucleus when it is initially created either as the parent isotope of interest in a compound nucleus reaction or as the daughter in an α-decay sequence. This can be illustrated by considering the case of ^{289}Fl. From Table VI, we see that in the decay from ^{293}Lv, the [707]15/2$^-$ ground state of ^{289}Fl is populated preferentially. In turn, this state shows a fine structure in its decay to states of the daughter, ^{285}Cn. However, if the ^{289}Fl were created as a compound nucleus reaction product, one would expect both the ground state and, at least, one of the positive-parity states to be populated (and to be an isomeric excited state—see Table V). Therefore, we may have additional α transitions from the excited state in ^{289}Fl adding more complexity to the decay scenarios and not necessarily allowing a simple interpretation of the α decays of the same nucleus when created by different processes.

V. SUMMARY

In this article, we have applied the superfluid tunneling model to compare against the experimental data on known α decays of odd-A and odd-odd SHN with $Z \geqslant 100$ and

$A \geqslant 250$. We have found a remarkable quantitative agreement between the data and the results of our calculations. The agreement is at a level that is comparable to empirical parametrizations exemplified by comparison with the Viola-Seaborg formula and the Royer formula.

We have used the STM to examine the influence of quasiparticle structure on the properties of the chains of α decays arising from the decay of odd-A SHN. There are many other sets of calculations of the one-quasi-particle structure of odd-A superheavy nuclei using various phenomenological and self-consistent mean-field models, and our paper is not meant to be an exhaustive comparison. There have even been previous qualitative efforts to understand the effect of the quasiparticle structure on the α decay [57,58]. Using a model, such as the STM, helps identify features in the α-decay fine structure, which might be used to discriminate between theoretical descriptions. Using representative calculations, available in the literature [15,45,48–50], of the one-quasi-particle structure of nuclei in the decay chains of ^{289}Mc ($Z = 115$, $N = 174$) and ^{293}Lv ($Z = 116$, $N = 177$), we illustrate the important role played by opposite-parity high-Ω orbitals in defining the observed characteristics of the α-decay chains. We point out sources of possible ambiguities that may arise due to the quasiparticle structure when assigning α-decay chains to specific SHN.

Given the potential for the quasiparticle structure to influence the characteristics of the α decay, it is quite remarkable that the agreement among the experimental data, the STM, and the empirical formulas is as good as it appears. This seems to be in large part due to the fact that most of the experimental data to date are thought to involve α transitions between states with the same (or similar) spins and parities. It will be interesting to see if the role of the quasiparticle structure, and particularly the influence of the high-Ω orbitals, is identified as more data becomes available. There does appear to be some evidence of this in the most recent experiments on the fine structure seen in the ^{289}Fl decay chains [16,17]. Also, it will be important to account for possible decay chains with different characteristics arising from the same isotope [59] and to experimentally determine the Z [13,14] and A [60] of the SHN. We hope that investigations such as ours will contribute to the interpretation of such future experiments.

APPENDIX: SUPERFLUID TUNNELING MODEL

The Schrödinger equation for the model can be written as

$$\left(-\frac{\hbar^2}{2D}\frac{\partial^2}{\partial \xi^2} + V(\xi)\right)\psi(\xi) = E\psi(\xi). \quad \text{(A1)}$$

ξ is a generalized deformation variable describing the path of the system in the multidimensional space of deformations. In the case of only quadrupole deformation, this would mean that ξ is proportional to the axial deformation parameter β_2. The parent nucleus evolves from a configuration with a small deformation $\xi \approx 0$ to the touching configuration of daughter-plus-α particle at $\xi = 1$.

Equation (A1) can be discretized on a mesh of n steps such that $\Delta \xi = 1/n$. One can then derive the expression for the inertial mass parameter as

$$D = -\frac{\hbar^2}{2v} n^2. \tag{A2}$$

v is the transition matrix element between two successive steps. For α decay, $n = 4$ is assumed [35,38]. The transition matrix element is governed by a pairing operator and is estimated using the Bardeen-Cooper-Schrieffer model such that

$$v = -\left(\frac{\Delta_n^2 + \Delta_p^2}{4G} \right) \tag{A3}$$

$G = 25/A$ MeV is the standard pairing strength and $\Delta_n = \Delta_p = \Delta = 12A^{-1/2}$ MeV are the pair gap parameters.

The decay constant λ can be calculated in terms of the α-particle formation probability P, the assault frequency of the particle against the barrier (also known as the knocking frequency) f and the transmission coefficient of the α particle through the barrier T_L such that

$$\lambda = PfT_L. \tag{A4}$$

To calculate P, we use the wave function of the ground state of a harmonic-oscillator $V(\xi) = \frac{1}{2}C\xi^2$ such that $P = |\psi(\xi = 1)|^2$ with

$$\psi(\xi) = \left(\frac{\alpha}{\sqrt{\pi}} \right)^{\frac{1}{2}} e^{-\frac{1}{2}\alpha^2\xi^2}, \tag{A5}$$

where

$$\alpha^2 = \sqrt{\frac{C}{2|v|}} n. \tag{A6}$$

The potential-energy parameter, $C = 2V(\xi = 1) = 2(U_N + U_C - Q_\alpha)$ with U_N and U_C being the nuclear potential (for which we used the Christensen-Winther potential [61]) and the Coulomb potential, respectively. The details of the potential parameters used can be found in Ref. [36]. The assault frequency can then be calculated via the formula $f = \omega/2\pi$, where $\omega = \sqrt{C/D}$.

Finally, the transmission coefficient T_L for the α particle to tunnel through the Coulomb barrier starting from the daughter-α touching configuration is given by

$$T_L = \frac{\rho}{F_L^2(\eta, \rho) + G_L^2(\eta, \rho)}, \tag{A7}$$

where $\rho = R_0 k$ with $k = \sqrt{2\mu Q_\alpha}/\hbar$ (μ is the reduced mass) and $R_0 = 1.2(A_D^{1/3} + A_\alpha^{1/3}) + 0.63$ fm, and $\eta = 1/ka$ where $a = \hbar^2/(e^2 \mu Z_D Z_\alpha)$. Here, F_L and G_L are the regular and irregular Coulomb functions [62], which take into account the additional centrifugal barrier when the orbital angular momentum L of the emitted α particle is nonzero.

[1] K. Morita *et al.*, J. Phys. Soc. Jpn. **73**, 2593 (2004).
[2] Y. T. Oganessian *et al.*, Phys. Rev. Lett. **83**, 3154 (1999).
[3] Y. T. Oganessian *et al.*, Phys. Rev. C **69**, 021601(R) (2004).
[4] Y. T. Oganessian *et al.*, Phys. Rev. C **63**, 011301(R) (2000).
[5] Y. T. Oganessian *et al.*, Phys. Rev. Lett. **104**, 142502 (2010).
[6] Y. T. Oganessian *et al.*, Phys. Rev. C **74**, 044602 (2006).
[7] K. Morita, Nucl. Phys. A **944**, 30 (2015).
[8] Y. T. Oganessian and V. K. Utyonkov, Nucl. Phys. A **944**, 62 (2015).
[9] S. Hofmann *et al.*, Eur. Phys. J. A **10**, 5 (2001).
[10] D. Ackermann, Prog. Theor. Phys. Suppl. **196**, 255 (2012).
[11] D. Ackermann, Nucl. Phys. A **944**, 376 (2015).
[12] Y. T. Oganessian, Phys. Rev. C **87**, 014302 (2013).
[13] D. Rudolph *et al.*, Phys. Rev. Lett. **111**, 112502 (2013).
[14] J. M. Gates *et al.*, Phys. Rev. C **92**, 021301(R) (2015).
[15] Y. Shi, D. E. Ward, B. G. Carlsson, J. Dobaczewski, W. Nazarewicz, I. Ragnarsson, and D. Rudolph, Phys. Rev. C **90**, 014308 (2014).
[16] A. Såmark-Roth, Ph.D. thesis, Spectroscopy along Decay Chains of Element 114, Flerovium, Lund University, 2021.
[17] D. M. Cox, A. Såmark-Roth *et al.*, Phys. Rev. C **107**, L021301 (2023).
[18] B. Buck, A. C. Merchant, and S. M. Perez, Phys. Rev. C **45**, 2247 (1992).

[19] B. A. Brown, Phys. Rev. C **46**, 811 (1992).
[20] C. Xu and Z. Ren, Nucl. Phys. A **753**, 174 (2005).
[21] C. Xu and Z. Ren, Phys. Rev. C **74**, 014304 (2006).
[22] P. Mohr, Phys. Rev. C **73**, 031301(R) (2006).
[23] D. Ni and Z. Ren, Phys. Rev. C **83**, 014310 (2011).
[24] K. P. Santhosh, S. Sahadevan, and J. G. Joseph, Nucl. Phys. A **850**, 34 (2011).
[25] Y. Qian, Z. Ren, and D. Ni, Phys. Rev. C **89**, 024318 (2014).
[26] V. Y. Denisov, O. I. Davidovskaya, and I. Y. Sedykh, Phys. Rev. C **92**, 014602 (2015).
[27] J. G. Deng, J. C. Zhao, P. C. Chu, and X. H. Li, Phys. Rev. C **97**, 044322 (2018).
[28] D. Bai and Z. Ren, Phys. Rev. C **103**, 044316 (2021).
[29] D. N. Poenaru and R. A. Gherghescu, Phys. Rev. C **97**, 044621(2018).
[30] D. S. Delion, Z. Ren, A. Dumitrescu, and D. Ni, J. Phys. G: Nucl. Part. Phys. **45**, 053001 (2018).
[31] A. Dumitrescu and D. S. Delion, At. Data Nucl. Data Tables **145**, 101501 (2022).
[32] Z. Wang and Z. Ren, Phys. Rev. C **106**, 024311 (2022).
[33] F. Barranco, R. A. Broglia, and G. F. Bertsch, Phys. Rev. Lett. **60**, 507 (1988).
[34] F. Barranco, E. Vigezzi, and R. A. Broglia, Phys. Rev. C **39**, 2101 (1989).

[35] F. Barranco, G. Bertsch, R. Broglia, and E. Vigezzi, Nucl. Phys. A**512**, 253 (1990).

[36] J. Rissanen, R. M. Clark, A. O. Macchiavelli, P. Fallon, C. M. Campbell, and A. Wiens, Phys. Rev. C **90**, 044324 (2014).

[37] R. M. Clark and D. Rudolph, Phys. Rev. C **97**, 024333 (2018).

[38] D. M. Brink and R. A. Broglia, *Nuclear Superfluidity* (Cambridge University Press, Cambridge, UK, 2005).

[39] V. E. Viola and G. T. Seaborg, J. Inorg. Nucl. Chem. **28**, 741 (1966).

[40] A. Parkhomenko and A. Sobiczewski, Acta Phys. Pol., B **36**, 3095 (2005).

[41] G. Royer, Nucl. Phys. A **848**, 279 (2010).

[42] G. Audi and A. H. Wapstra, Nucl. Phys. A **595**, 409 (1995).

[43] NNDC, Evaluated Nuclear Structure Data File Database, http://www.nndc.bnl.gov/ensdf/.

[44] D. Rudolph *et al.*, in *Nuclear Structure and Dynamics'15*, edited by M. Lipoglavšek, M. Milin, T. Nikšić, S. Szilner, and D. Vretenar, AIP Conf. Proc. No. 1681 (AIP, Melville, NY, 2015), p. 030015.

[45] U. Forsberg *et al.*, Nucl. Phys. A **953**, 117 (2016).

[46] D. Kaji *et al.*, J. Phys. Soc. Jpn. **86**, 085001 (2017).

[47] J. Khuyagbaatar *et al.*, Phys. Rev. C **99**, 054306 (2019).

[48] B. G. Carlsson and I. Ragnarsson, Phys. Rev. C **74**, 011302(R) (2006).

[49] A. Parkhomenko and A. Sobiczewski, Acta Phys. Pol., B **35**, 2447 (2004).

[50] S. Ćwiok, W. Nazarewicz, and P. H. Heenen, Phys. Rev. Lett. **83**, 1108 (1999).

[51] J. Dobaczewski, A. V. Afanasjev, M. Bender, L. M. Robledo, and Y. Shi, Nucl. Phys. A **944**, 388 (2015).

[52] S. Ćwiok, P. H. Heenen, and W. Nazarewicz, Nature (London) **433**, 705 (2005).

[53] I. Ahmad *et al.*, Phys. Rev. C **87**, 054328 (2013).

[54] I. Ahmad, J. P. Greene, F. G. Kondev, and S. Zhu, Phys. Rev. C **91**, 044310 (2015).

[55] D. Ni and Z. Ren, Phys. Rev. C **86**, 054608 (2012).

[56] D. Ni and Z. Ren, Phys. Rev. C **87**, 027602 (2013).

[57] A. N. Kuzmina, G. G. Adamian, and N. V. Antonenko, Phys. Rev. C **85**, 027308 (2012).

[58] V. G. Kartavenko *et al.*, Chinese Phys. C **41**, 074105 (2017).

[59] U. Forsberg *et al.*, Phys. Lett. B **760**, 293 (2016).

[60] J. M. Gates *et al.*, Phys. Rev. Lett. **121**, 222501 (2018).

[61] R. A. Broglia and A. Winther, *Heavy Ion Reactions* (Addison-Wesley, New York, 1991).

[62] R. Thomas, Prog. Theor. Phys. **12**, 253 (1954).